Electronic Supplementary Material (ESI) for Journal of Materials Chemistry A.

Supplementary Materials

Efficient Cycling Utilization of Solar-Thermal Energy for Thermochromic Display with Controllable Heat Output

Weixiang Yang,[a] Yiyu Feng*,[a, c, d] Qianyu Si,[a] Qinghai Yan,[a] Peng Long,[a] Liqi Dong,[a] Linxia Fu,[a] and Wei Feng*[a, b, c, d]

Preparation of tri-Azo molecules

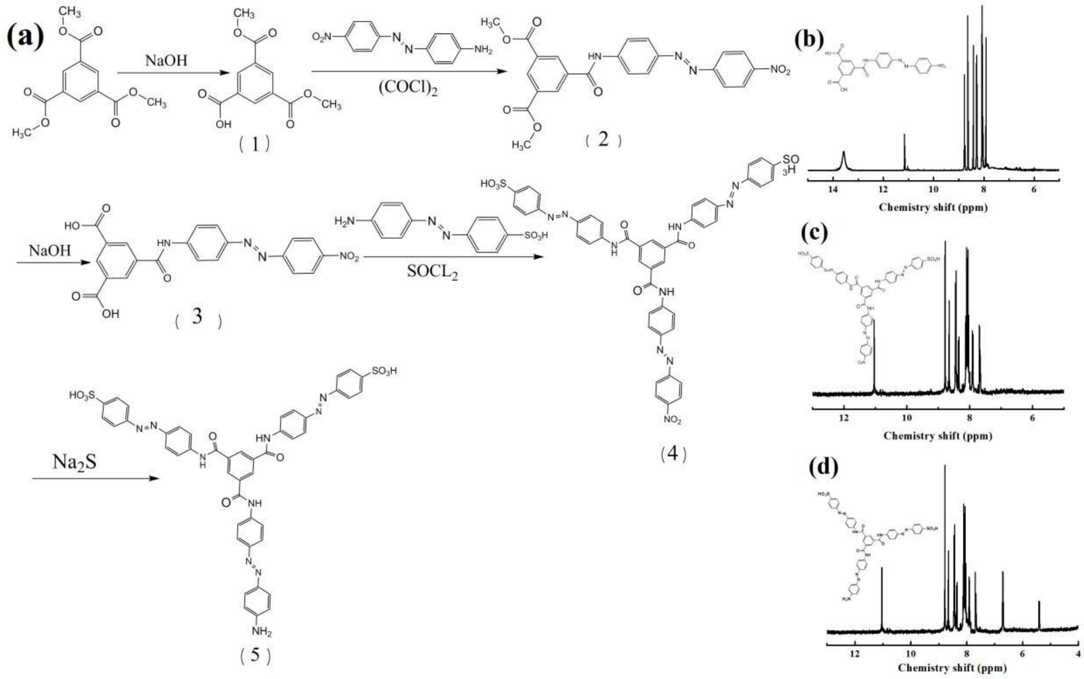

Figure S1. Experimental procedure for tri-Azo

3,5-bis(methoxycarbonyl)benzoic acid (1)

We prepared product 1 according to the literature with minor modifications.[1] Trimethyl benzene-1,3,5-tricarboxylate (3.7815 g, 15 mmol) and NaOH (0.5798 g, 14.8 mmol) were dissolved in methanol (300 mL) while stirring, then we slowly heating it to the reflux temperature and stirred for 12 h. The solvent was removed under reduced pressure, and dichloromethane (200 mL) was added to dissolve the solids. The product was extracted by adding saturated $NaHCO_3$ solution (600 mL), the aqueous phase was separated and washed two times with dichloromethane, and then acidified to pH=1 with 10% hydrochloric acid to yield a precipitate. The precipitate was collected and washed with distilled water until pH=7. The white powder we obtained was dried in a vacuum oven to give product 1. The yield was 80% (2.856 g).

^1H NMR (300 MHz, DMSO-d6) δ (ppm)=13.71 (s, 1H), 8.64(s, 2H), 8.62 (s, 1H), 3.93 (s, 6H)

Compound (2)

To a solution of compound 1 (2.856 g, 12 mmol) in acetonitrile (100 mL), 1.78 mL $(COCL)_2$ (1.2 equivalent to compound 2) and 50 μL DMF was added at 0 ℃ under nitrogen and then stirred for 4 h at 20 ℃. Then, Disperse Orange 3 (2.9 g, 12 mmol) and 4.18 mL triethylamine (30 mmol) was added to the solution. The reaction mixture was stirred at 0 ℃ for 10 h, and then poured into water to precipitate the product. The precipitate was collected and washed with dilute HCl (pH ≈ 2), then aqueous $NaHCO_3$ (pH ≈ 9), and finally distilled water. The obtained solid was then dried at 60 ℃ in vacuo to give the desired compound 2 as an orange powder. The yield was 90% (4.99 g). ^1H NMR (300 MHz, DMSO-d6) δ (ppm) = 10.99 (s, 1H), 8.80 (d, 2H), 8.65 (t, 1H), 8.06 (d, 2H), 7.96 (d, 2H), 7.88 (d, 2H), 7.60 (t, 1H), 7.58 (t, 2H） .

Compound-3 (3)

Compound 2(4.62 g, 10.0 mmol) was dissolved in a mixture of 150 mL tetrahydrofuran and 50 mL water, then 2.5 equiv of NaOH(1.0 g, 25 mmol) to 2 was dissolved in 40 mL H_2O and then slowly added to the above mixture, drop by drop. The resulting solution was stirred for 10 h at reflux temperature. After the completion of the reaction, the solvent (THF) was removed by rotoevaporation under reduced pressure. The residue was then re-dissolved in large quantities of water, which was then acidified to pH=2 with aqueous HCl to generate a precipitate. The precipitate was filtered and washed with distilled water until pH=7. The finally obtained solid was dried in vacuum oven to give product 3. The yield was 95% (4.12 g). ^{1}H NMR (300 MHz, DMSO-d6) δ (ppm)=13.59 (s, 2H), 10.96 (s, 1H), 8.76 (d, 2H), 8.65 (t, 1H), 8.43 (d, 2H), 8.27 (d, 2H), 8.08 (d, 2H), 7.93 (t, 1H).

Tri-Azo$_{\mathbf{NO2}}$ (4)

To a solution of compound 3 (3.9 g, 9 mmol) in dichloromethane (100 mL), 2.68 mL $(COCL)_2$ (2.4 equiv to compound 2) and 100 μL DMF was added at 0 °C under nitrogen and then stirred for 4 h at 20 °C. Then, 4-aminoazobenzene-4-sulfonic acid (5 g, 18 mmol) and 4.18 mL triethylamine (30 mmol) was added to the solution. The reaction mixture was stirred at 0 °C for 40 h, after which the excess solvent (DCM) was removed in vacuo by rotoevaporation, and the concentrated solution was precipitated with diethyl ether. The precipitate was collected and washed three times with a diethyl ether/dichloromethane (1/1, volume ratio) mixture. The crude product was dried in a vacuum oven, and then re-dissolved in distilled water and reprecipitated in HCl water at 0 °C. The precipitate was collected and dried at 60 °C in a vacuum oven until it reached a constant weight. The yield was 60% (5.14 g, 5.4 mmol) ^{1}H NMR (300 MHz, DMSO-d6) δ (ppm)=10.59 (s, 3H), 8.78 (s, 3H), 8.63 (d, 4H), 8.42 (d, 6H), 8.05 (d, 6H), 7.85 (d, 6H), 7.58 (t, 3H).

Tri-Azo$_{\mathbf{NH3}}$ (5)

Compound 4 (4.76 g, 5.0 mmol) was dissolved in a mixture of 100 mL water and 30 mL dimethyl formamide, and then $NaS \cdot 9H_2O$ (2.4 g, 10 mmol) was dissolved in 100 mL H_2O and slowly added to the above mixture, drop by drop. The resulting solution was stirred for 36 h at reflux temperature. After removing the solvents, H_2O was added to the solid and the pH was adjusted to 8 with 30% aqueous NH_3 solution. The aqueous layer was then extracted with dichloromethane. The dichloromethane layer was collected and dried over anhydrous Na_2SO_4. The solvent was evaporated under a vacuum to obtain triAzo with a yield of 45%.

Synthesis of rGO

According to the literature, we prepared GO through the acid oxidation of flake graphite. GO dispersed in water (1 mg mL^{-1}) was adjusted to pH=9 by adding 5 wt% sodium carbonate solution, and the partial reduction of GO (rGO) was carried out using 30 mL of sodium borohydride solution (20 mg mL^{-1}) at 85 ºC for 2 h. By mean of centrifugation, filtration, and rinsing with distilled water several times we obtained the rGO, which combined both good dispersibility and a degree of conjugate structure.

Synthesis of tri-Azo/rGO

TriAzo (1.84 g, 2 mmol) and $NaNO_2$ (0.152 g, 2.2 mmol) were dissolved in 40 mL di-water at room temperature, which was then slowly dripped into the HCl solution (10 mL, 1 mol L^{-1}) in an ice bath to form diazonium salt in 1 h. This diazonium salt solution was slowly added to the above rGO solution (100 mL, 1 mg mL^{-1}). The reaction continued for 6 h at 0–5 °C and then held at room temperature overnight. The mixture was then washed with distilled water, acetone, and DMF several times to remove the remaining azobenzene derivative molecule and excessive diazonium salts. The resulting solid was collected until the filtrate showed no characteristic absorption band in the UV-Vis spectra. Finally, tri-Azo/rGO was obtained by drying in a vacuum overnight at 70 ºC.

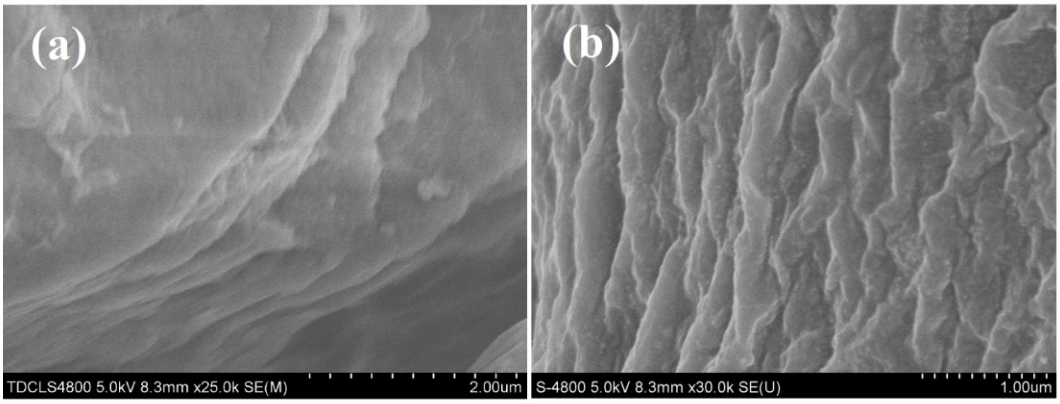

Figure S2. SEM of (a) rGO and (b) tri-Azo/rGO. Mono-layer rGO retains a smooth silk-like structure with the size of 10 μm^2 after the reduction. After the grafting of Azo molecules, the roughness of tri-Azo/rGO increased because of its being covered by many organic addends.

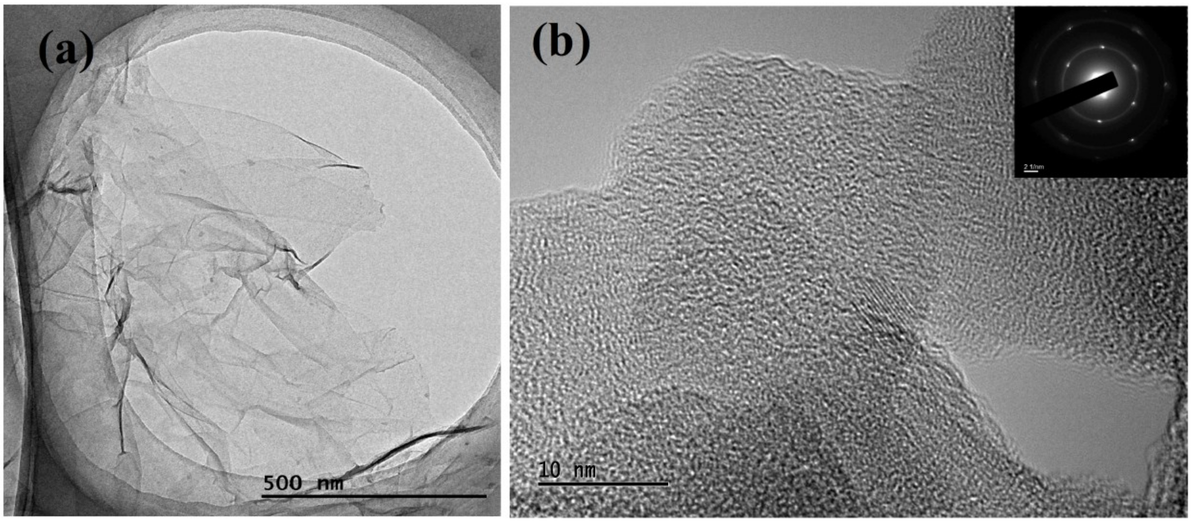

Figure S3. TEM images of rGO. (a) Low-resolution images of rGO. (b) high resolution images of rGO.

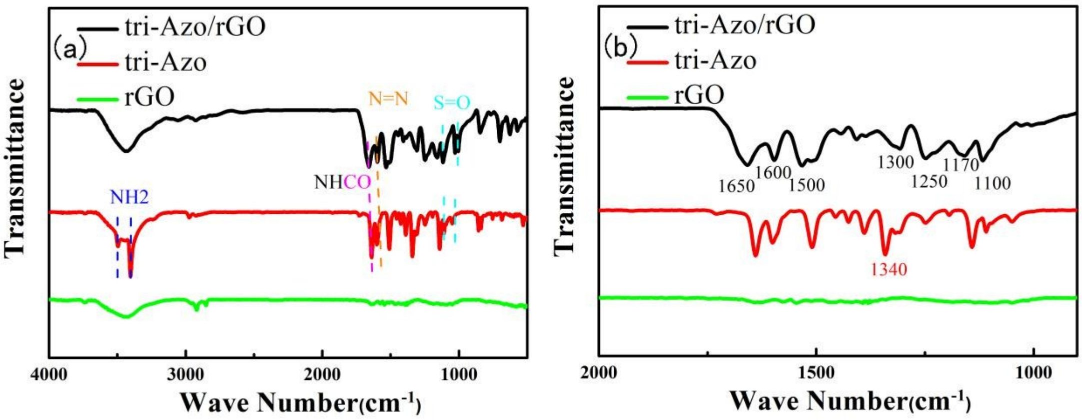

Figure S4. (a) FTIR spectra of rGO, tri-Azo and tri-Azo/rGO. (b) The 2000-1000 cm^{-1} region of FTIR spectra (**Figure S4** b).

The bands at 3523 cm^{-1} and 3383 cm^{-1} are attributed to -NH_2 for tri-Azo/rGO, and the peak at 1600cm^{-1} and 1650 cm^{-1} belongs to N=N stretching and C=O of –NHCO-, respectively.[2] The band corresponding to S=O stretching of -SO_3H were found at 1170 cm^{-1} and 1100 cm^{-1}.[3] The peaks at 1500 cm^{-1} (C=C stretching of benzene)[2], 1340 cm^{-1} (C-N stretching of -NH_2)[4, 5], 1300 cm^{-1} (C-H stretching) and 1250 cm^{-1} (C-C stretching) are also observed.

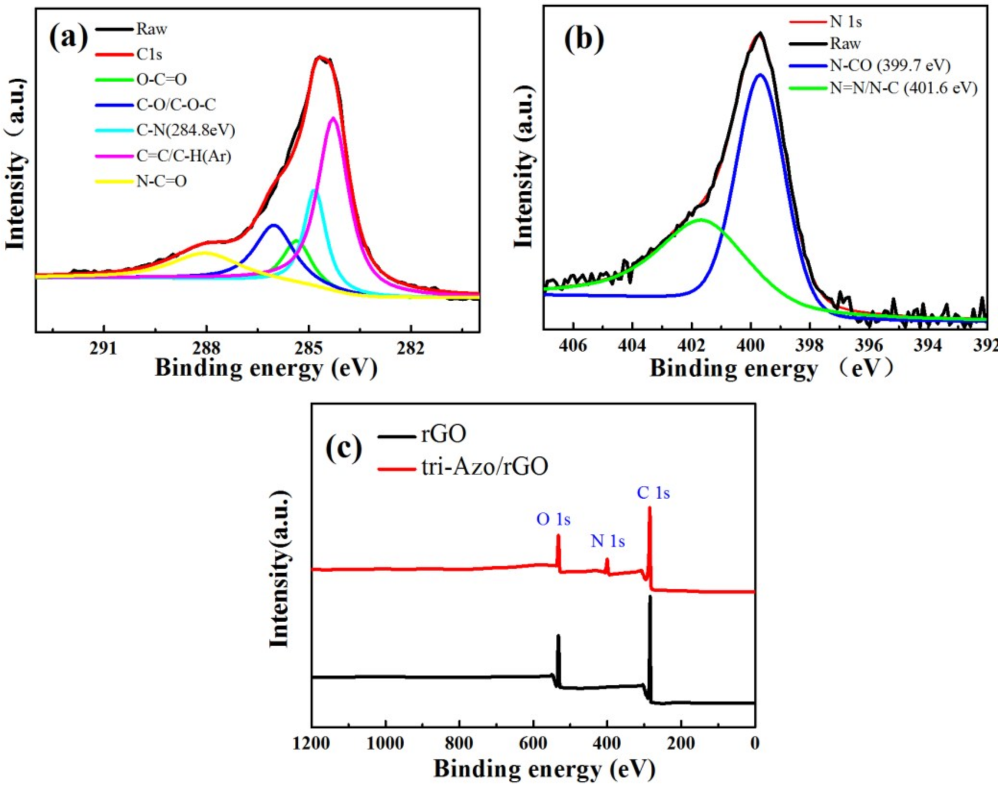

Figure S5. (a) C1 region in XPS spectra of tri-Azo/rGO, (b) N1 region in tri-Azo/rGO and (c) Wide-scan survey XPS spectra of tri-Azo/rGO. The existed of C-N, O-C-O confirmed the tri-Azo graft onto the rGO.

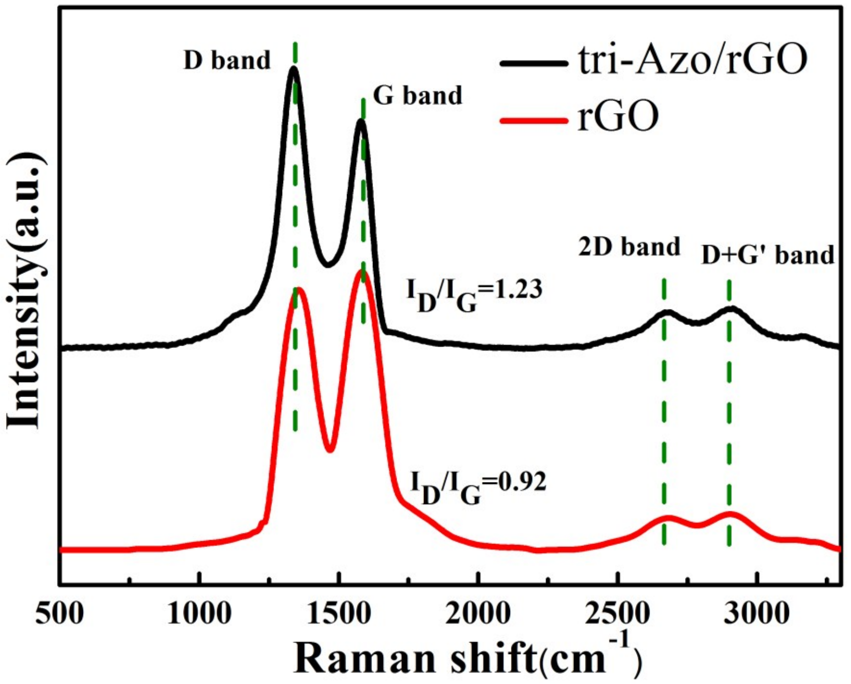

Figure S6. Raman spectrum of rGO, tri-Azo/rGO. Compared with that of RGO, I_D/I_G of tri-Azo/rGO shows significant increases.

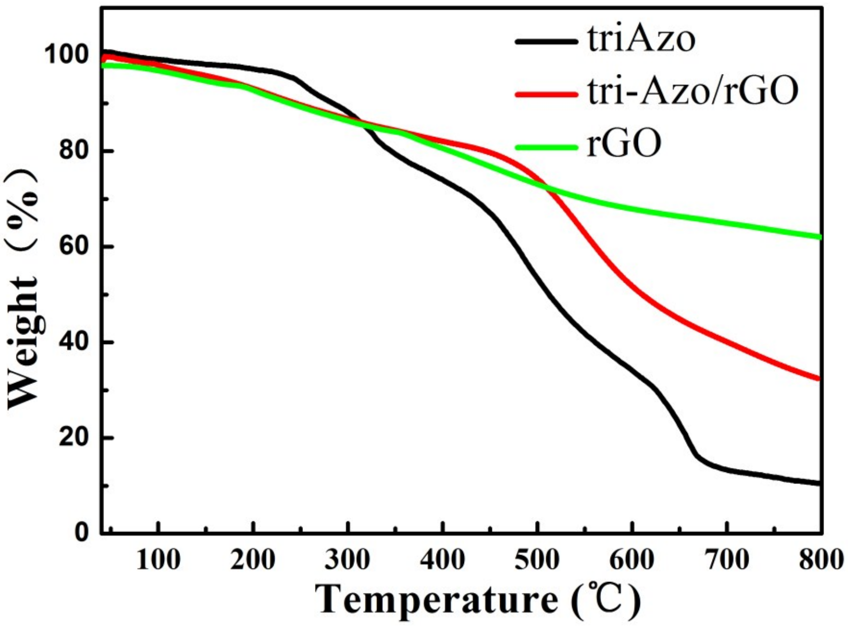

Figure S7. TGA result of tri-Azo/rGO.

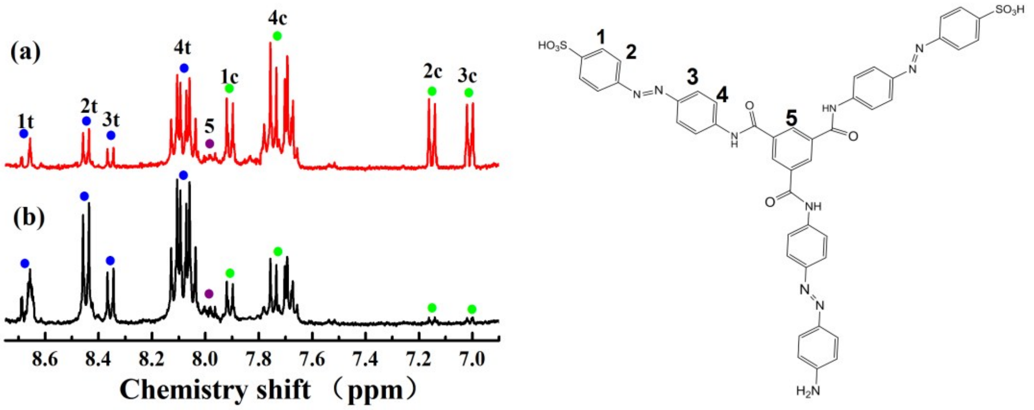

Figure S8. ^{1}H-NMR of (a) tri-Azo after UV (365 nm) irradiation for 10 min. (b) tri-Azo before UV irradiation.

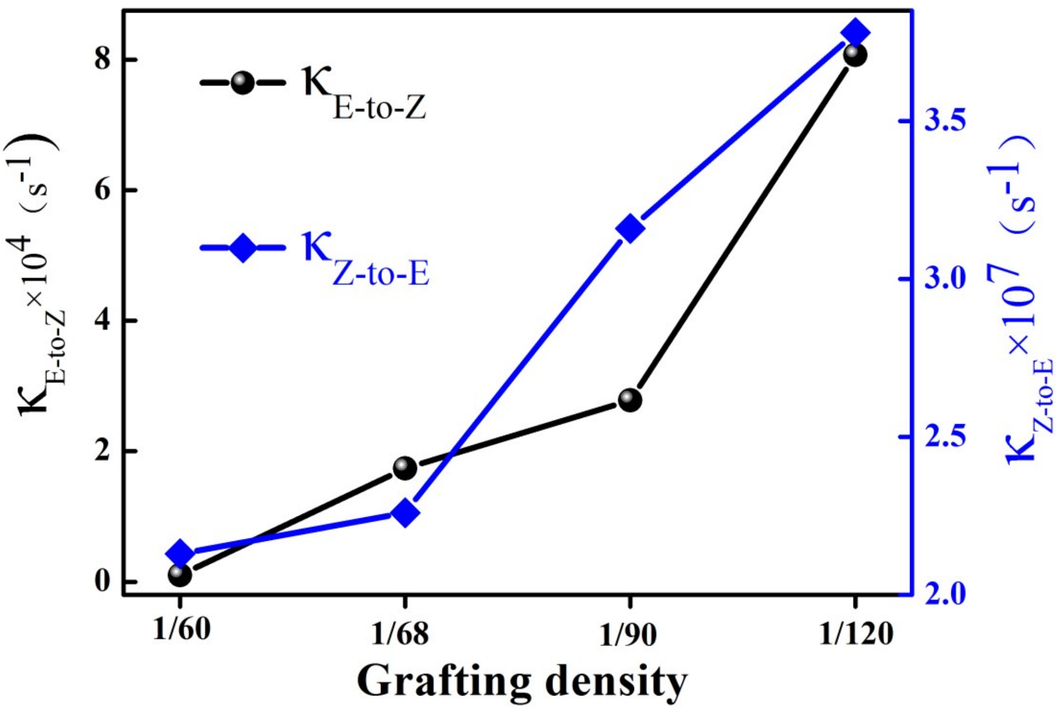

Figure S9. κ_{rev} and κ_{iso} of tri-Azo/rGO in different grafting density.

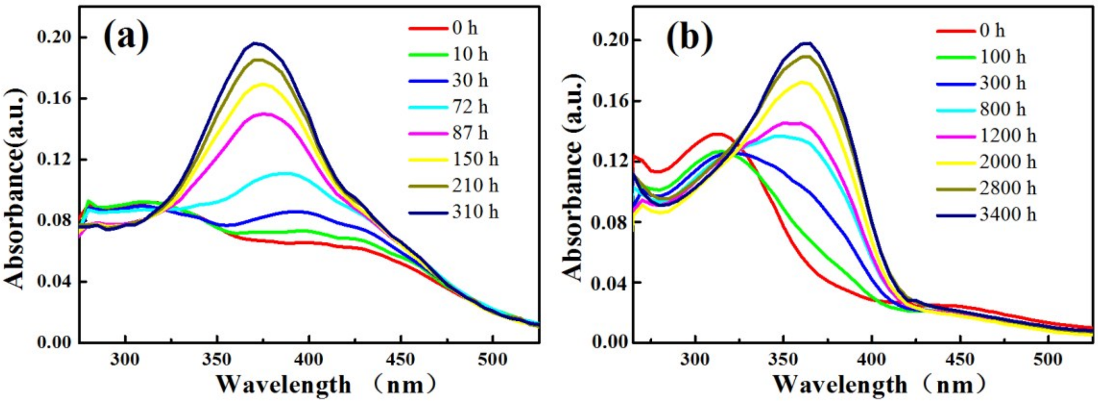

Figure S10. Time-evolved absorption spectra of (a) tri-Azo and (b) tri-Azo/rGO in the darkness after irradiation.

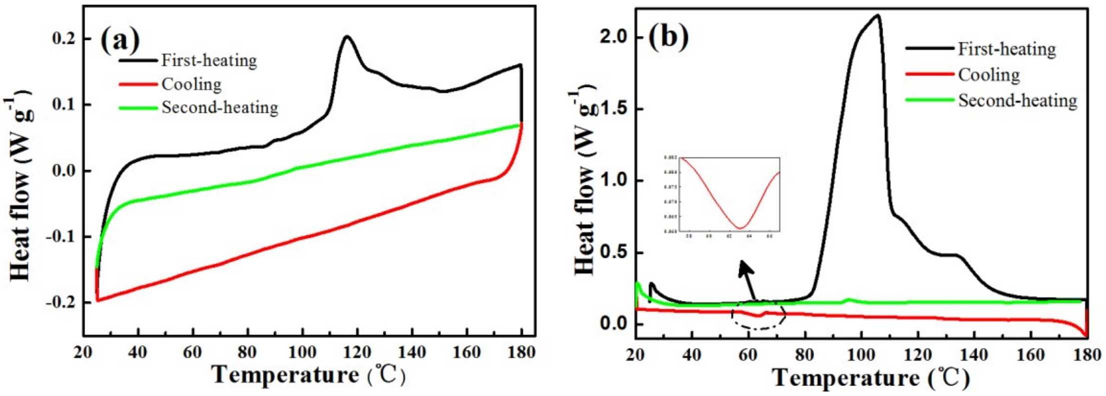

Figure S11. DSC traces of (a) tri-Azo and (b) tri-Azo/rGO in the *Z*-rich photo-stationary states after irradiation by UV light with the first heating, cooling, and second heating segments at 20 ºC min^{-1} and 10 ºC min^{-1}, respectively. The weak endothermic peak during the first cooling indicates the formation of H-bonds between the two adjacent *E*-tri-Azo molecules.

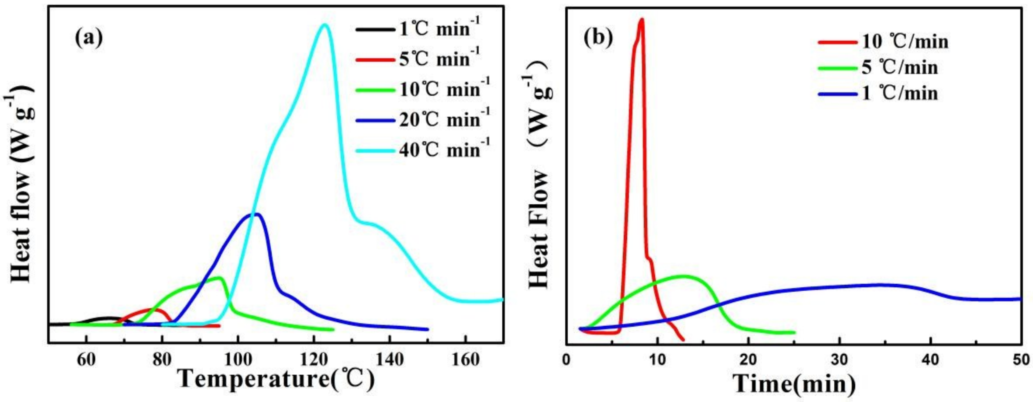

Figure S12. DSC traces of tri-Azo/rGO (a) Temperature-Heat flow curve of tri-Azo/rGO at different heating rate(1, 5, 10, 20 and 40 ℃ min^{-1}). (b) Time-Heat flow curve of tri-Azo/rGO at different heating rate (1, 5 and 10 min^{-1})

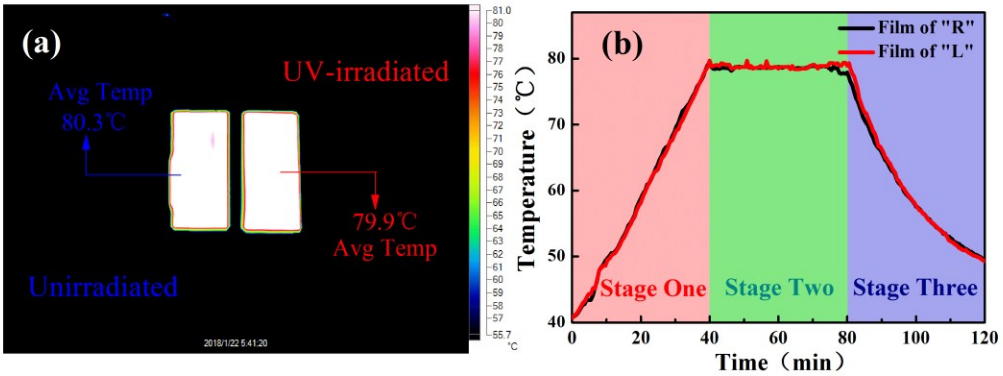

Figure S13. Top-view IR heat map and average temperature of tri-Azo/rGO films with no UV light absorbed. (a) two tri-Azo/rGO films without UV light irradiated and (b) no temperature difference formed in the process.

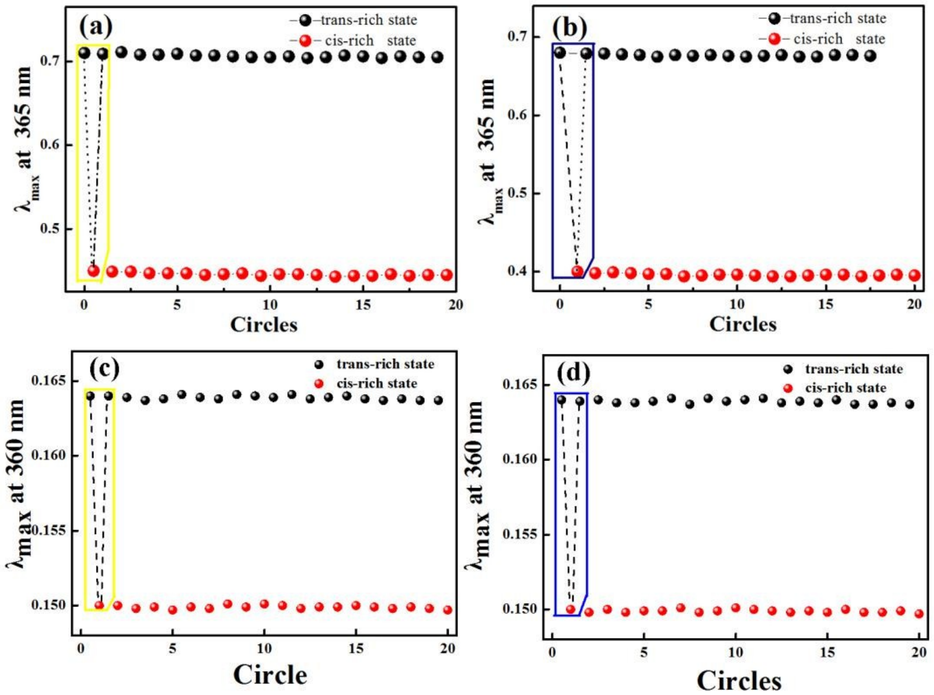

Figure S14. Cycling stability of *E*-*Z*-*E* isomerization of Solution(a) and the film(c) of rGO–triAzo induced by alternately irradiating UV light(365 nm) and blue light (430 nm); the solution(b) and film(d) of rGO–triAzo induced by alternately irradiating UV light(365 nm) and heat(80 ℃), show excellent cycling stability of *E*-*Z*-*E* isomerization for 100 cycles without obviously degradation.

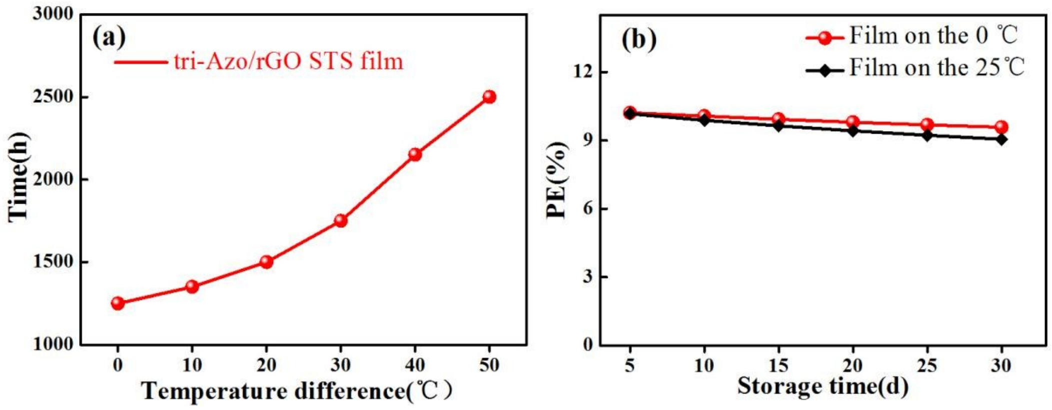

Figure S15. (a) Time required to release half of the heat stored in STS film with different temperature differences ($\Delta T = T_e - T_a$ ， T is the temperature of the film or the systems, T_a is the ambient temperature). (b) PE of STS film after storage for 5–30 days at 0 °C and 25 °C.

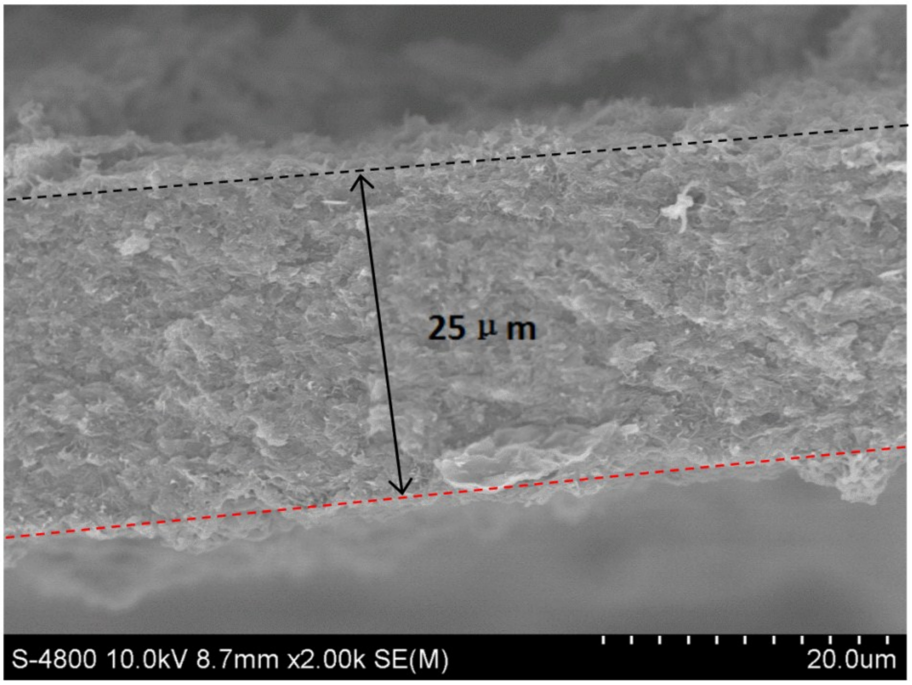

Figure S16. Cross-sectional SEM image of a solid-state PTF film.

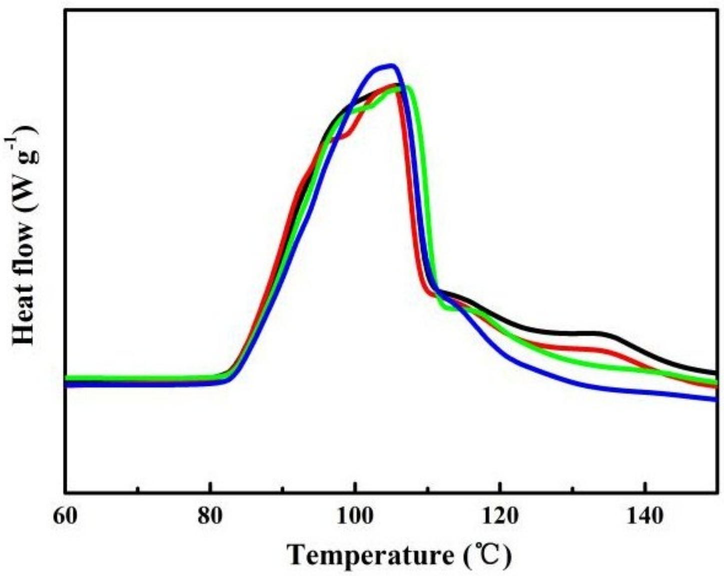

Figure S17. DSC measurement repeated 4 times in the same sample

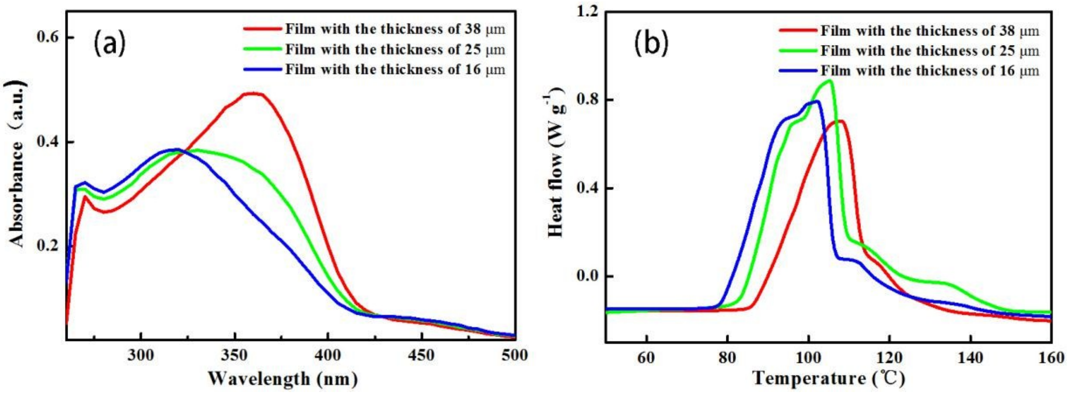

Figure S18. The Time-evolved absorption spectra (a) and DSC traces (b) of the tri-Azo/rGO film with different thickness under same charging time.

S19 Table

Table S1. TGA and XPS data of tri-Azo/rGO

	TGA			XPS		
	D_t (%)			Element content		D_f
	700	750	800	C	N	
rGO	65.2	64.3	63.5			
tri-Azo	19.2	17.6	16.7			
tri-Azo/rGO	46.3	45.9	44.8	75.6	4.1	1:120
	43.1	42.8	42.0	67	4.5	1:90
	40.8	39.5	38.7	55.6	4.4	1:68
	39.4	38.1	37.3	79.2	6.7	1:60

Dt is residual weight percentage

Table S2. $\kappa_{E\text{-to-}Z}$, $\kappa_{Z\text{-to-}E}$, isomerization and $\tau_{1/2}$ of tri-Azo/rGO

	Solution		Powder		
D_f	$\kappa_{E\text{-to-}Z}$ (s^{-1})	$DI_{E\text{-to-}Z}$ (%)	$\kappa_{Z\text{-to-}E}$ (s^{-1})	$DI_{Z\text{-to-}E}$(%)	$\tau_{1/2}$（h）
1/60	1×10^{-5}	53.5	2.13×10^{-7}	85.4	1300
1/68	1.74×10^{-4}	72.6	2.26×10^{-7}	87.9	1250
1/90	2.78×10^{-4}	76.4	3.16×10^{-7}	91.5	1170
1/120	8.07×10^{-4}	83.0	3.78×10^{-7}	93.7	1100

Df is grafting density of triAzo/rGO; $\kappa_{E\text{-to-}Z}$ is the first-order rate constant of trans-to-cis; $DI_{E\text{-to-}Z}$ is the degree of trans-to-cis; $\kappa_{Z\text{-to-}E}$ is the first-order rate constant of cis-to-trans; $DI_{Z\text{-to-}E}$ is the degree of cis-to-trans.

Table S3. Heat release of tri-Azo$_{1:68}$/rGO film for different heating rates

	Heating rate (°C min^{-1})			
	0.5	1	5	40
Exothermic time (min)	45-50	20-23	3-5	1-2
Energy density (Wh kg^{-1})	150.2	149.6	145.4	98.7
ΔT_{max} (℃)	1.6	6.3	8.2	12.1

Table S4. Power density of tri-Azo/rGO in different conditions

Grafting density	Blue light (W kg^{-1})	Heating rate (W kg^{-1})	
		10 °C min^{-1}	40 °C min^{-1}
1/60	26.5	1250.8	2682.9
1/68	30.0	1371.7	3036.9
1/90	24.9	1099.0	2302.8
1/120	18.9	805.1	1701.3

Table S5. Energy density of tri-Azo/rGO for different heating rates

Grafting density	Energy density (Wh kg^{-1})			
	1 °C min^{-1}	10 °C min^{-1}	20 °C min^{-1}	40 °C min^{-1}
1/60	137.9	135.5	114.1	89.4
1/68	150.2	148.6	125.4	98.7
1/90	112.2	109.9	87.5	76.8
1/120	75.4	73.8	61.7	53.9

Table S6. $DI_{Z\text{-to-}E}$ of tri-Azo/rGO under different external stimuli

	Grafting density	Dark	Blue light (430 nm)	1 °C min^{-1}	10 °C min^{-1}	20 °C min^{-1}	40 °C min^{-1}
$DI_{Z\text{-to-}E}$	1/60	85.4%	90.9%	80.1%	69%	63.4%	50.8%
	1/68	87.9%	91.3%	85.9%	74.6%	66.9%	59.7%
	1/90	91.5%	93.2%	87.4%	82.5%	74.2%	66.3%
	1/120	93.7%	93.7%	89.9%	84.1%	79.8%	75.6%

$DI_{Z\text{-to-}E}$ is the degree of cis-to-trans.

Table S7. Heat-release of tri-$Azo_{1:68}$/rGO film for different heating rates

	$DI_{Z\text{-to-E}}$	Energy density (Wh kg^{-1})	Exothermic time (min)
1 °C/min	64%	108.3	23
10 °C/min	56.5%	98.6	6

$DI_{Z\text{-to-E}}$ is the degree of cis-to-trans.

Table S8 The time of the Z-to-E isomerization, half-lives and power density of tri-Azo/rGO film at different temperature.

Temperature (℃)	t (h)	$\boldsymbol{\tau}_{1/2}$ (h)	Power density (W kg^{-1}) (Blue-light irradiated)
0	18	1630	10
5	10	1500	14
25	6	1250	30

t is the UV irridiation time

Table S9. $DI_{Z\text{-to-}E}$ of tri-Azo/rGO in processes under Conditions Ⅰ and Ⅱ

	40 to 63 °C	63 °C for 23 min	40–77 °C	77 °C for 37 min
$DI_{Z\text{-to-}E}$ (%)	24.0	36.4	53.5	69.7

$DI_{Z\text{-to-}E}$ is the degree of cis-to-trans.

Table S10. The energy density of four DSC curves of tri-Azo$_{1:68}$/rGO

	1	2	3	4	Average
Energy density (Wh kg^{-1})	150.7	150.3	150.5	149.7	150.3

Table S11 Transmittance of tri-Azo/rGO film at different film thickness

Thickness of the film (μm)	16	25	38
Transmittance of UV (%)	5.546	3.973	2.433
$\mathrm{DI}_{\text{Z-to-E}}$ (%)	69.3	54.7	33.3

$\mathrm{DI}_{\text{Z-to-E}}$ (%) is the isomerization degree of the film with different thickness after the same charging time.

Table S12 Degree of isomerization of solution and powder under different UV-initiation times

$T_{\text{UV-irradiation}}$ (h)	0.2	1	3	6
DI_{solution} (%)	52.3	74.8	84.5	83
DI_{powder} (%)	11.3	39.6	64.7	72.6

$T_{\text{UV-irradiation}}$ is the time of UV-irradiation. DI_{solution} and DI_{powder} is the degree of isomerization of solution and powder

S20. Equations.

Equation S1

$$D_\mathrm{f} = \frac{R_\mathrm{p} - R}{R_\mathrm{p} - R_\mathrm{a}} \times 100\%$$

where R_a is the residual weight percentage of triAzo, R is the residual weight percentage of rGO–triAzo, R_p is the residual weight percentage of rGO.

Equation S2

$$D\mathrm{i} = \frac{A_\infty - A_0}{A_\mathrm{s} - A_0}$$

where D_i is the isomerization degree and A_0 is the theoretical absorption intensity of rGO–triAzo in the metastable state (*cis*-rich), irradiated by UV light, A_s is the experimental minimum absorption intensity of rGO–triAzo irradiated by UV, and A_∞ is the absorption intensity of rGO–triAzo before UV irradiation.

Equation S3

$$\ln\left(\frac{A_\infty - A_t}{A_\infty - A_0}\right) = -K_{rev}t$$

A_0 is the absorption intensity of rGO–triAzo in the metastable state (*cis*-rich) irradiated by UV light, A_t is the absorption intensity of rGO–triAzo reversing for "*t*" time and A_∞ is the absorption intensity of rGO–triAzo after complete *cis*-trans reversion.

Equation S4

$$\eta_{MOST} = \frac{\mathrm{n}_{DHA} \cdot \alpha_{VHF} \cdot \Delta H_{stor}}{A \cdot E_{AM1.5}}$$

Where n_{DHA} is the DHA1 flow speed in mol s^{-1}, α_{VHF} is the conversion ratio of DHA1 into VHF1 and A is the irradiated area in m^2

Equation S5

$$\eta_{comb} = \eta_{MOST} + \eta_{SWH} = \frac{n_{NBD} \cdot \alpha_{QC} \cdot \Delta H_{stor}}{A \cdot E_{AM1.5}} + \frac{m_{H_2O} \cdot C_{PH_2O} \cdot \Delta T}{A \cdot E_{AM1.5}}$$

η_{comb} is the combined efficiency of the device. η_{MOST} is the solar energy storage efficiency of the **molecular solar thermal energy storage** (MOST) system. η_{SWH} is the efficiency of the **solar water heating system** (SWH) system. Where α_{QC} is the measured conversion of **quadricyclane** (QC) after irradiation, ΔH_{stor} is the stored energy of QC (in J mol s^{-1}), n is the flow speed (in mol s^{-1}), A the irradiated area (in m^{-2}), and $E_{AM1.5}$ is the energy of incoming solar radiation (in W m^{-2}). m is the water flow-rate (in Kg s^{-1}), C_p is the heat capacity of water (J kg^{-1} K^{-1}), and ΔT is the measured temperature rise (in K).

References:

1. Y.-W. Hao, H.-Y. Wang, Y. J. Huang, B.-R. Gao, Q.-D. Chen, L.-B. Li and H.-B. Sun, *J. Mater. Chem. A*, 2013, 1, 5244.

2. Wang, B. Wu, S. Li, G. Sinawang, X. Wang and Y. He, *ACS Sustainable Chemistry & Engineering,* 2016, 4, 4036.

3. T. S. Jo, C. H. Ozawa, B. R. Eagar, L. V. Brownell, D. Han, C. Bae, *J. Polym. Sci. Part A,* 2009, 47, 485 – 496

4. X. Wang, J. Deng, X. Duan, D. Liu, J. Guo and P. Liu, J. Mater. Chem. A, 2014, 2, 12323

5. Z. Liu, H. Zhou, Z. Huang, W. Wang, F. Zeng and Y. Kuang, J. Mater. Chem. A, 2013, 1, 3454.